Electronic Supplementary Material (ESI) for ChemComm.

Isocyanide insertion into Au-H bonds: first gold iminoformyl complexes

Julio Fernandez-Cestau,* Luca Rocchigiani, Anna Pintus, Raquel J. Rama, Peter H. M. Budzelaar* and Manfred Bochmann

Supporting Information

1. Synthesis and characterization

When required, manipulations were performed using standard Schlenk techniques under dry nitrogen or an M. Braun glove box. Nitrogen was purified by passing through columns of supported P_2O_5 with moisture indicator, and activated 4 Å molecular sieves. Anhydrous solvents were freshly distilled from appropriate drying agents. IR spectra were recorded using a Perkin Elmer Spectrum 65 FT-IR spectrometer with a diamond ATR attachment. Elemental analyses were carried out at London Metropolitan University. The (C^N^C)AuH complexes were prepared following literature methods.[S1] The C≡NR ligands were purchased from Aldrich and used without further purification. AIBN (BDH Chemicals) was dried *in vacuo* and stored under N_2 in the glovebox prior to use. The Brønsted acid $[H(OEt_2)_2][H_2N\{B(C_6F_5)_3\}_2]$ (HAB_2) was prepared following literature methods.[S2] NMR solvents were degassed by three freeze-pump-thaw cycles and stored on activated 4 Å molecular sieves prior to use.H and $^{13}C\{^1H\}$ spectra were recorded using a Bruker Avance DPX-300 spectrometer. ^1H NMR spectra (300.13 MHz) were referenced to the residual protons of the deuterated solvent used. $^{13}C\{^1H\}$ NMR spectra (75.47 MHz) were referenced internally to the D-coupled ^{13}C resonances of the NMR solvent. Where applicable, resonances were assigned by using 2D COSY, HSQC and HMBC experiments.

Synthesis of (L^H)Au-(E)-CHNXyl (1a)

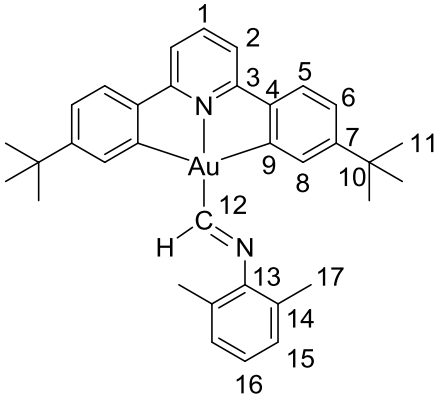

The (L^H)AuH (30 mg, 0.056 mmol), C≡NXyl (ca. 4 mg, 0.3 mmol), and AIBN (ca. 0.2 eq.) were dissolved in toluene and the reaction mixture kept at 60 °C for 2h. The volatile components were evaporated and the residue washed with CH_3OH and Et_2O and dried at vacuum. This produces (L^H)Au-(E)-CHNXyl (**1a**) as a pale-yellow solid (35 mg, 0.054 mmol, 96 %). Anal. Calcd for $C_{34}H_{37}N_2Au$·(670.65): C, 60.89; H, 5.56; N, 4.18. Found: C, 60.55; H, 5.70; N, 4.25. IR (cm^{-1}): ν(C=N) 1636 (w). ^{1}H NMR (CD_2Cl_2, 300.13 MHz, 298K): δ 9.54 (br, s, 1H, H^{12}), 7.89 (br, s, 2H, H^8), 7.81 (t, ^3J = 7.8 Hz, ^{1}H, H^1), 7.59 (d, ^3J = 7.9 Hz, 2H, H^5), 7.46 (d, ^3J = 7.8 Hz, 2H, H^2), 7.31 (br, d, $^3J \approx$ 7.9 Hz, 2H, H^6), 7.10 (d, ^3J = 6.9 Hz, 2H, H^{15}), 6.93 (t, ^3J = 6.9 Hz, 1H, H^{16}), 2.30 (s, 6H, H^{17}), *1.71 (s, AIBN impurity)*, 1.34 (s, 18H, H^{11}). ^{13}C{^{1}H} NMR(CD_2Cl_2, 75.47 MHz, 298K): 172.02 (s, C^{12}), 166.22 (s, C^9), 163.44 (s, C^3), 154.69 (s, C^7), 147.82 (s, C^4), 142.26 (s, C^1), 131.96 (s, C^8), 128.32 (s, C^{15}), 126.96 (s, C^{14}), 125.43 (s, C^5), 124.10 (s, C^6), 123.17 (s, C^{16}), 116.43 (s, C^2), 35.67 (s, C^{10}), 31.45 (s, C^{11}), 25.38 *(s, AIBN impurity)*, 19.12 (s, C^{17}).

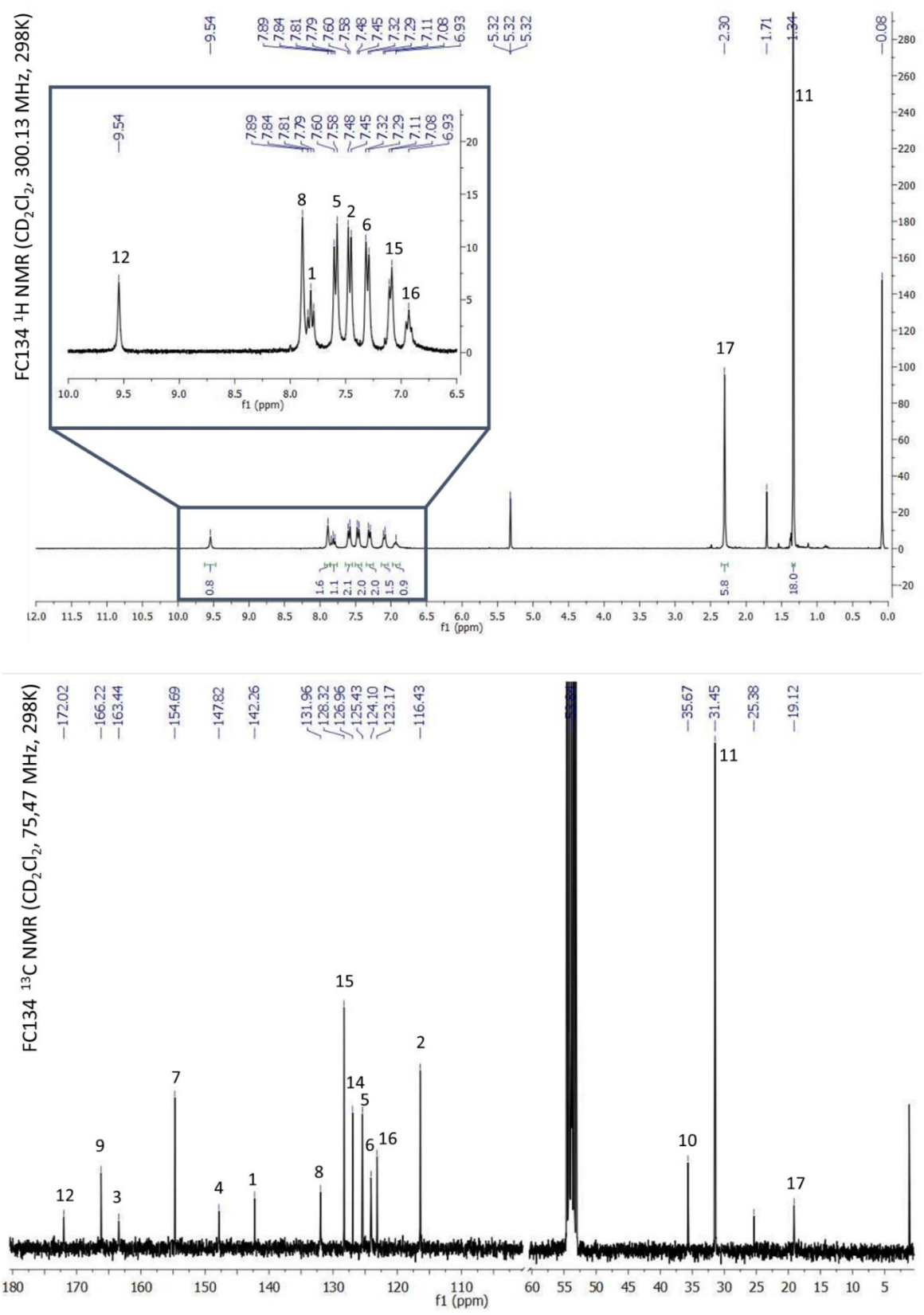

Figure S1.1: ^{1}HNMR (top) and ^{13}C{^{1}H} NMR (down) of complex (L^{H})Au-(E)-CHNXyl **1a** in CD_2Cl_2 at 298 K.

Synthesis of (L^{OMe})Au-(E)-CHNXyl (1b)

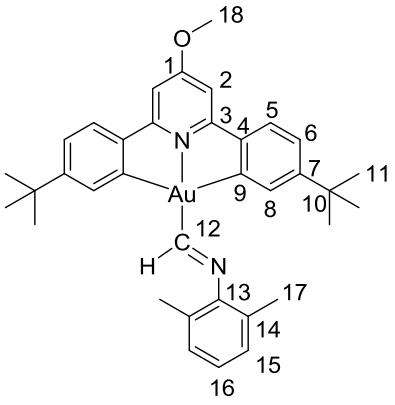

Following the procedure for **1a** but from (L^{OMe})AuH (30 mg, 0.053 mmol), C≡NXyl (ca. 4 mg, 0.3 mmol), and AIBN (ca. 0.2 eq.). Complex (L^{OMe})AuCHNXyl (**1b**) was isolated as a pale yellow solid (36 mg, 0.052 mmol, 98%). Anal. Calcd for $C_{35}H_{39}N_2AuO$·(700.68): C, 60.00; H, 5.61; N, 4.00. Found: C, 59.95; H, 5.60; N, 4.15. IR (cm^{-1}): ν(C=N) 1635 (w). ^{1}H NMR (CD_2Cl_2, 300.13 MHz, 298 K): δ 9.46 (br, s, 1H, H^{12}), 7.86 (br, s, 2H, H^8), 7.47 (d, ^3J = 7.9 Hz, 2H, H^5), 7.26 (d, ^3J = 7.9 Hz, 2H, H^6), 7.08 (d, ^3J = 7.0 Hz, 2H, H^{15}), 6.93 (t, ^3J = 7.0 Hz, 1H, H^{16}), 6.83 (s, 2H, H^2), 3.95 (s, 3H, H^{18}), 2.31 (s, 6H, H^{17}), 1.33 (s, 18H, H^{11}). $^{13}C\{^1H\}$ NMR(CD_2Cl_2, 75.47 MHz, 298K): 172.95 (s, C^{12}), 170.86 (s, C^1), 166.15 (s, C^9), 164.75 (s, C^3), 155.77 (s, C^{13}), 154.37 (s, C^7), 147.75 (s, C^4), 131.80 (s, C^8), 128.27 (s, C^{15}), 126.95 (s, C^{14}), 125.03 (s, C^5), 123.82 (s, C^6), 123.07 (s, C^{16}), 102.48 (s, C^2), 56.49 (s, C^{18}), 35.61 (s, C^{10}), 31.46 (s, C^{11}), 19.17 (s, C^{17}).

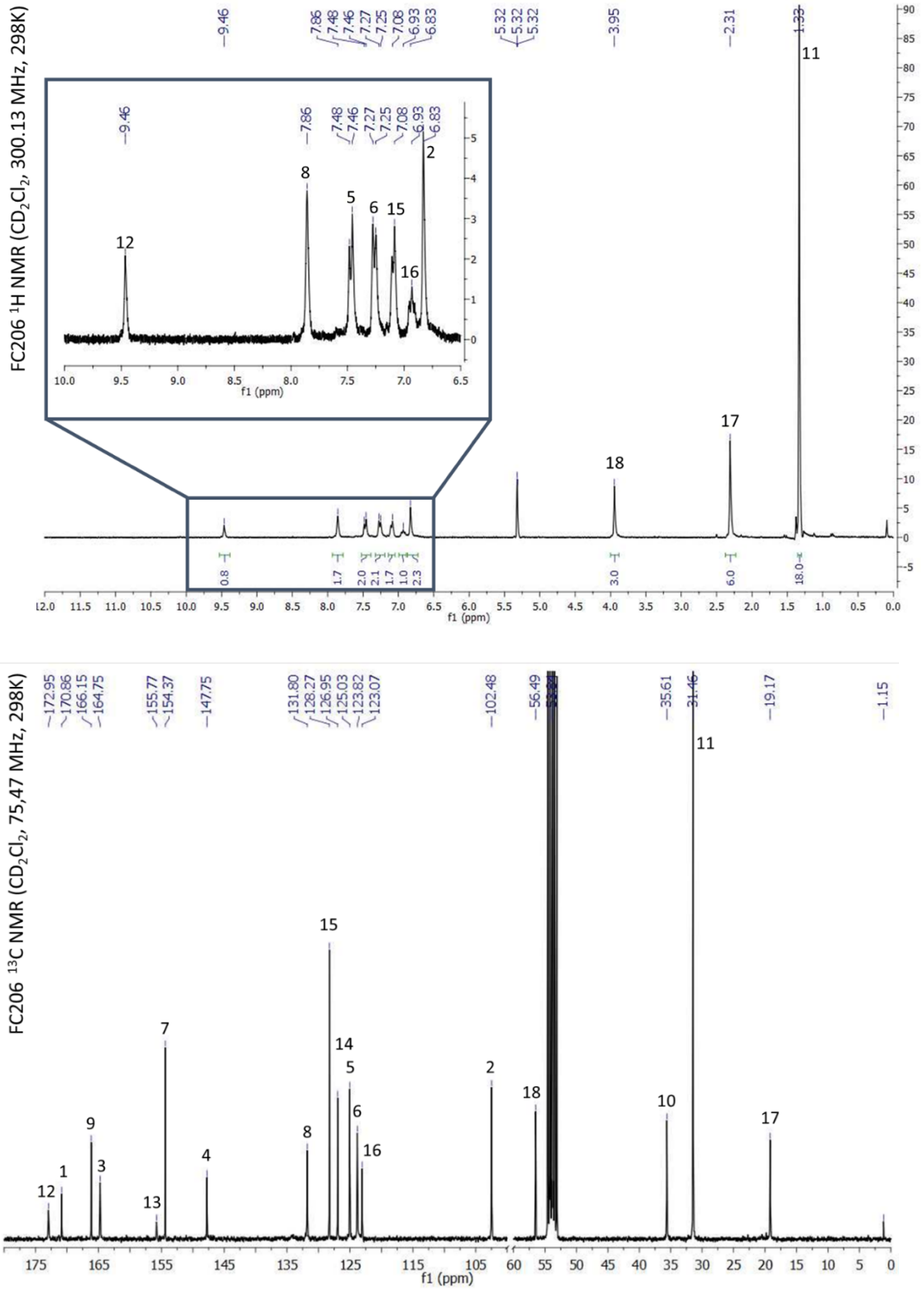

Figure S1.2: ^{1}HNMR (top) and ^{13}C{^{1}H} NMR (down) of complex (L^{OMe})Au-(E)-CHNXyl **1b** in CD_2Cl_2 at 298 K.

Synthesis of (L^H)Au-(*E, Z*)-CHNC$_6$H$_4$OMe-4 (2a)

Following the procedure for **1a** but from (L^H)AuH (30 mg, 0.056 mmol), C≡NC$_6$H$_4$OMe-4 (ca. 4 mg, 0.3 mmol), and AIBN (ca. 0.2 eq.). Complex (L^H)AuCHNC$_6$H$_4$OMe-4 (**2**) was isolated as a pale yellow solid (30 mg, 80%). Anal. Calcd for $C_{33}H_{35}N_2AuO\cdot$(672.62): C, 58.93; H, 5.25; N, 4.16. Found: C, 58.43; H, 5.10; N, 4.74. IR (cm^{-1}): ν(C=N) 1613 (br, w). ^{1}H NMR (CD_2Cl_2, 300.13 MHz, 298K): δ 9.85 (br, s, H^{12Z}), 9.80 (br, s, H^{12E}), 7.93 (d, ^4J = 1.6 Hz, H^{8Z}), 7.77 (t, ^3J = 8.0 Hz, H^{1E}, overlapped with ~7.79, H^{1Z}), 7.60 (d, ^3J = 8.2 Hz, H^{5Z}), 7.54-7.52 (overlap of aromatic signals), 7.42 (d, ^3J = 8.0 Hz, H^{2E}, overlapped with ~7.45, H^{2Z}), 7.32 (dd, ^3J = 8.2 Hz, ^4J = 1.8 Hz, H^{6Z}), 7.25-7.21 (overlap of aromatic signals), 6.97 (d, ^3J = 8.7 Hz, $H^{14Z\text{ or }15Z}$), 6.69 (d, ^3J = 8.7 Hz, $H^{14E\text{ or }15E}$), 3.84 (s, H^{17Z}), 3.64 (s, H^{17E}), 1.39 (s, H^{11Z}), 1.31 (s, H^{11E}). Using the relative integration of the signals H^{17Z}/H^{17E} and H^{11Z}/H^{11E} we estimate a Z/E ratio of about 1/7. $^{13}C\{^1H\}$ NMR(CD_2Cl_2, 75.47 MHz, 298K): 169.68 (s, C^{12Z}), 168.38 (s, C^{12E}), 166.55 (s, C^Z), 164.86 (s, $^4C^E$), 163.40 (s, C^Z), 162.88 (s, $^4C^E$), 157.88 (s, C^Z), 156.90 (s, $^4C^E$), 154.87 (s, $^4C^E$), 154.50 (s, C^Z), 147.84 (s, C^Z), 147.50 (s, $^4C^E$), 142.22 (s, C^{1Z}), 142.06 (s, C^{1E}), 134.42 (s, C^{8E}), 131.68 (s, C^{8Z}), 125.43 (s, C^{5E}), 125.33 (s, C^{5Z}), 124.19 (s, C^Z), 123.61 (s, $C^{6E\text{ or }14E\text{ or }15E}$), 121.83 (s, $C^{6E\text{ or }14E\text{ or }15E}$), 121.71 (s, C^Z), 116.43 (s, C^{2Z}), 114.60 (s, C^Z), 113.88 (s, $C^{14E\text{ or }15E}$), 55.83 (s, C^{17Z}), 55.47 (s, C^{17E}), 35.69 (s, C^{10Z}), 35.39 (s, C^{10E}), 31.42 (s, C^{11Z}), 31.33 (s, C^{11E}), 25.37 (*s, AIBN impurity*).

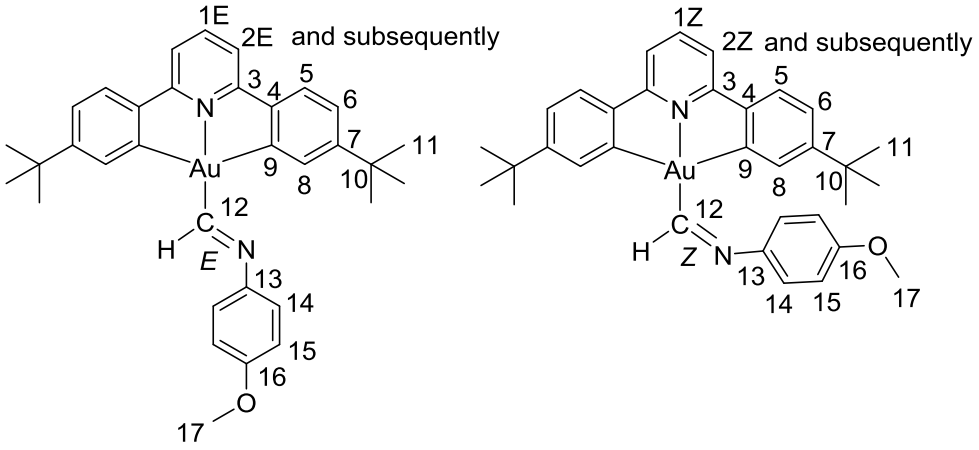

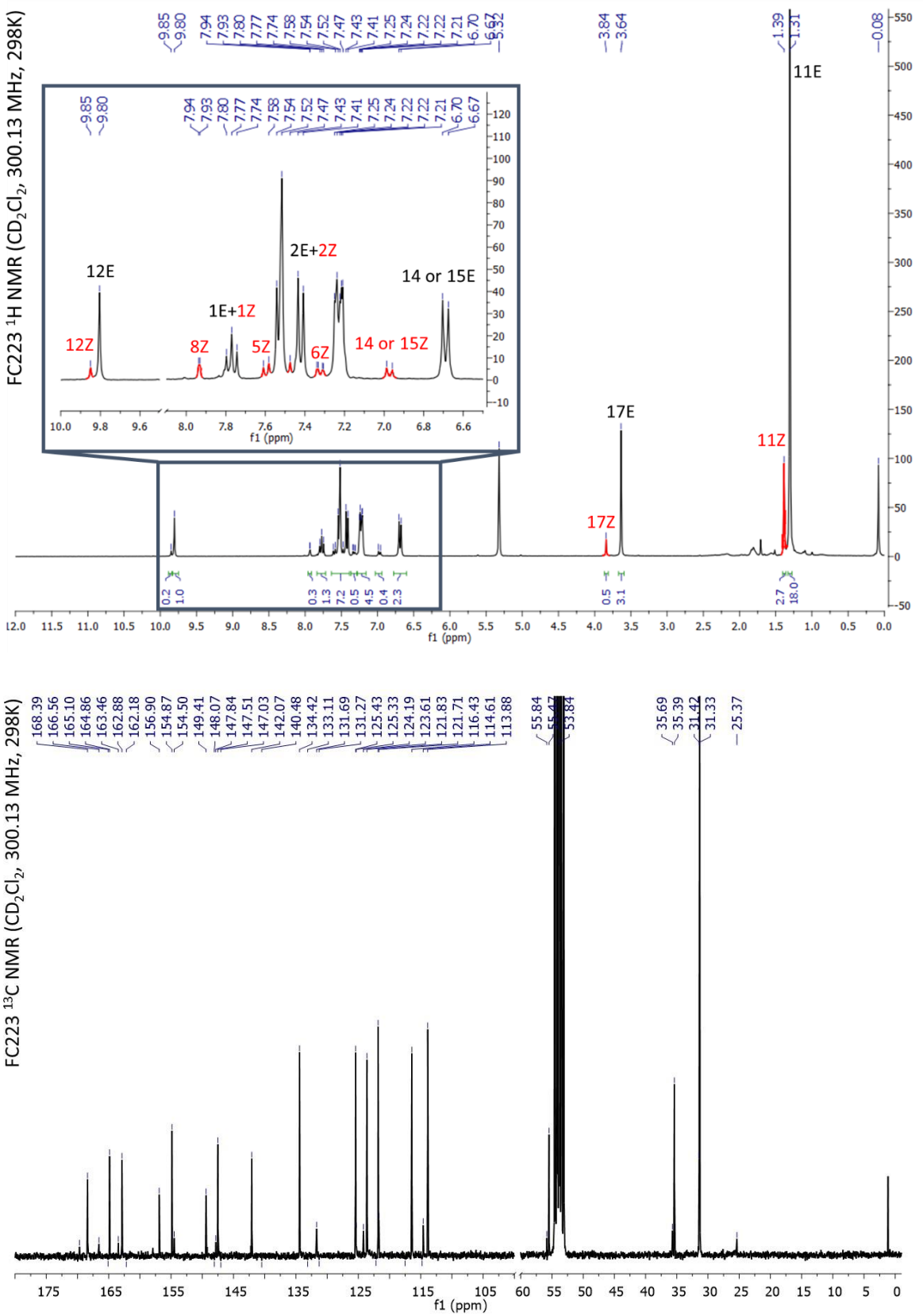

Figure S1.3: ^{1}HNMR (top) and $^{13}C\{^{1}H\}$ NMR (down) of complex (L^{H})Au-(E, Z)-$CHNC_6H_4OMe$-4 **2a** in CD_2Cl_2 at 298 K.

Synthesis of (L^H)Au-(E)-CHNC_6H_4(COOMe)-4 (3a)

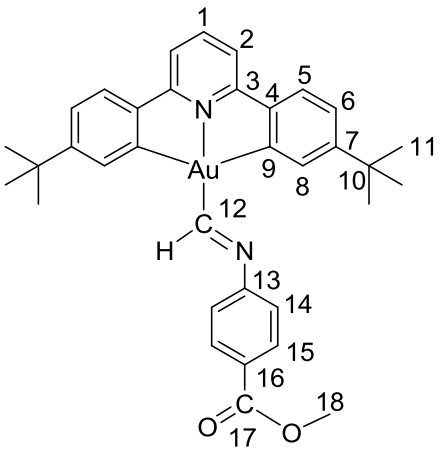

Following the procedure for **1a** but from (L^H)AuH (30 mg, 0.056 mmol), C≡NC_6H_4(COOMe)-4 (ca. 4 mg, 0.3 mmol), and AIBN (ca. 0.2 eq.). Complex (L^H)AuCHNC_6H_4(COOMe)-4 (**3**) was isolated as a pale yellow solid (33 mg, 85%). Anal. Calcd for $C_{34}H_{35}AuN_2O_2$·(700,63): C, 58.29; H, 5.04; N, 4.00. Found: C, 58.43; H, 5.10; N, 3.74. IR (cm^{-1}): ν(C=O) 1714 (s), ν(C=N) 1622 (w). ^{1}H NMR (CD_2Cl_2, 300.13 MHz, 298K): δ 9.88 (s, 1H, H^{12}), 7.78 (d, ^3J = 8.5 Hz, 2H, H^{15}), 7.70 (t, ^3J = 7.9 Hz, 1H, H^1), 7.55 (d, ^4J = 1.7 Hz, 1H, H^8), 7.48 (d, ^3J = 8.2 Hz, 1H, H^5), 7.34 (d, J = 7.9 Hz, 2H, H^2), 7.23 (dd, ^3J = 8.2 Hz, ^4J = 1.7 Hz, 2H, H^6), 7.18 (d, ^3J = 8.5 Hz, 2H, H^{14}), 3.74 (s, 3H, H^{18}), 1.34 (s, 18H, H^{11}). ^{13}C{^{1}H} NMR(CD_2Cl_2, 75.47 MHz, 298K): δ 172.36 (s, C^{12}), 167.04 (s, *^4C*), 164.55 (s, *^4C*), 162.91 (s, *^4C*), 160.33 (s, *^4C*), 154.94 (s, *^4C*), 147.42 (s, *^4C*), 142.16 (s, C^1), 134.37 (s, C^8), 130.47 (s, C^{15}), 125.97 (s, C^{17}), 125.53 (s, C^5), 123.72 (s, C^6), 120.48 (s, C^{14}), 116.47 (s, C^2), 52.01 (s, C^{18}), 35.42 (s, C^{10}), 31.35 (s, C^{11}).

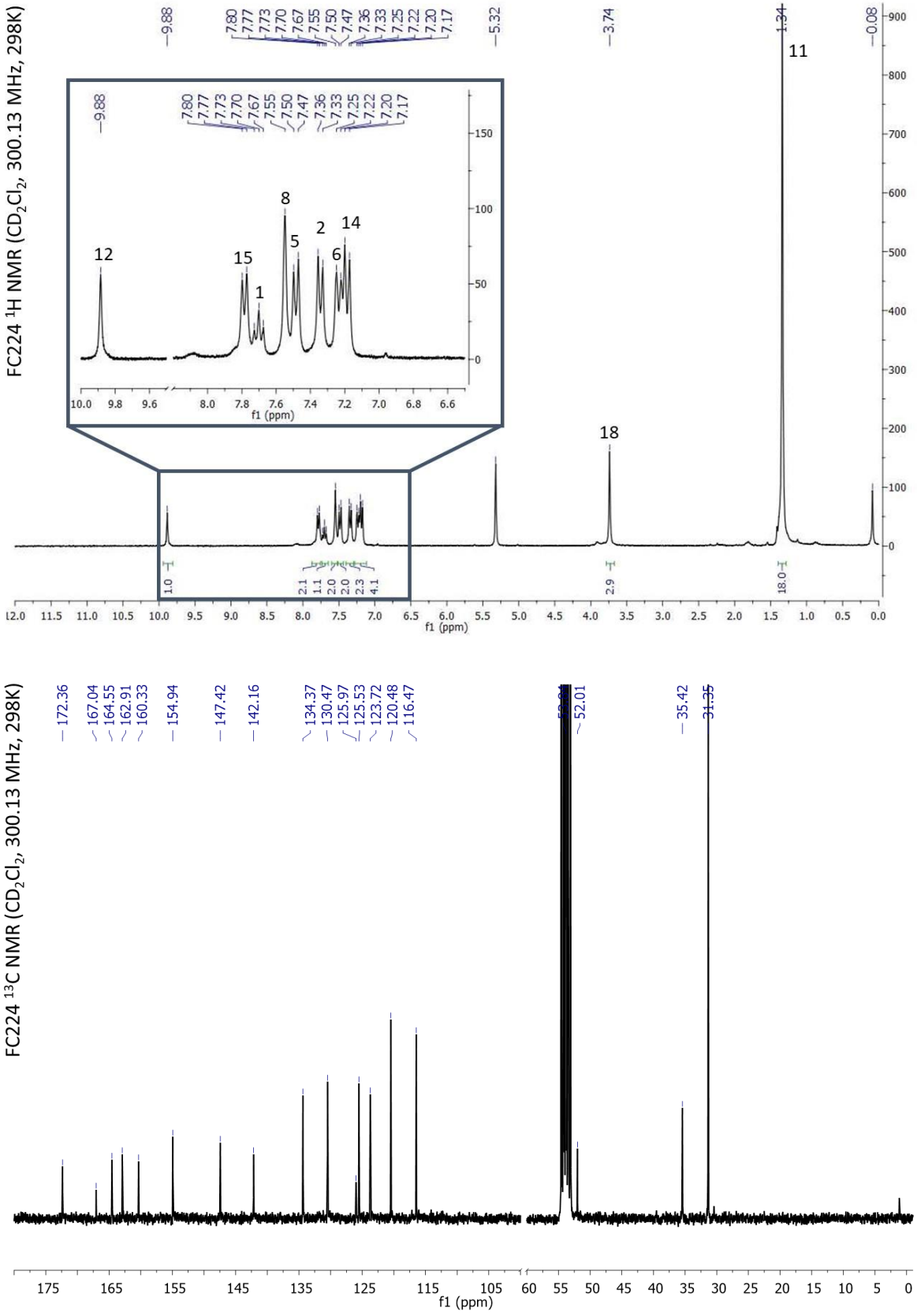

Figure S1.4: ^{1}HNMR (top) and $^{13}C\{^{1}H\}$ NMR (down) of complex (L^{H})Au-(E)-$CHNC_6H_4(COOMe)$-4 **3a** in CD_2Cl_2 at 298 K.

Synthesis of [(L^H)Au-(E, Z)-CHNHXyl][NH_2{$B(C_6F_5)_3$}$_2$]· 2 Et_2O (4a)

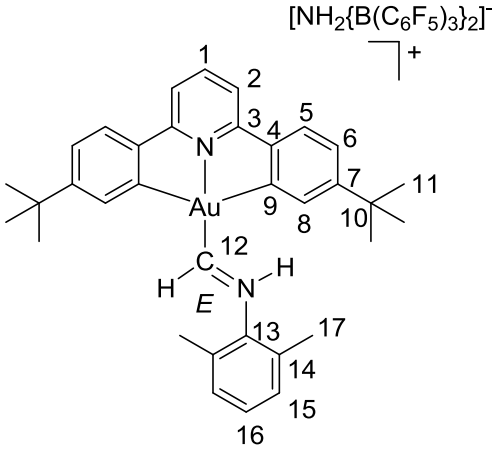

To a solution of (L^H)Au-(E)-CHNXyl in CD_2Cl_2 one equivalent of $H(OEt_2)_2NB_2$ is added what affords the quantitative formation of [(L^H)Au-(E)-CHNHXyl]H_2N{$B(C_6F_5)_3$}$_2$. ^{1}H NMR (CD_2Cl_2, 300.13 MHz, 298K): δ 11.56 (br, s, 1H, NH), 10.76 (d, ^3J = 19.6 Hz, 1H, H^{12}), 8.02 (t, ^3J = 8.0 Hz, 1H, H^1), 7.68 (d, ^3J = 8.4 Hz, 1H, H^5), 7.58 (d, J = 8.0 Hz, 2H, H^2), 7.51-7.45 (m, 5H, H^8+H^{15}+H^{16}) 7.39 (br, d, 2H, H^6), 5.60 (br, s, 2H, H_2N{$B(C_6F_5)_3$}$_2$), 3.47 (q, J = 7.0 Hz, 8H, -CH_2-, Et_2O), 2.58 (s, 3H, H^{17}), 1.32 (s, 18H, H^{11}), 1.15 (t, J = 7.0 Hz, 12H, -CH_3-, Et_2O). ^{13}C{^{1}H} NMR(CD_2Cl_2, 75.47 MHz, 298K): 208.77 (s, C^{12}), 164.50 (s, C^9), 164.27 (s, C^3), 157.04 (s, C^7), 146.77 (s, C^4), 144.40 (s, C^1), 133.06 (s, C^8), 131.85 (s, C^{15}), 131.71 (s, C^{14}), 130.73 (s, C^5), 127.01 (s, C^6), 126.13 (s, C^{16}), 117.89 (s, C^2), 35.88(s, C^{10}), 31.29 (s, C^{11}), 18.92 (s, C^{17}).

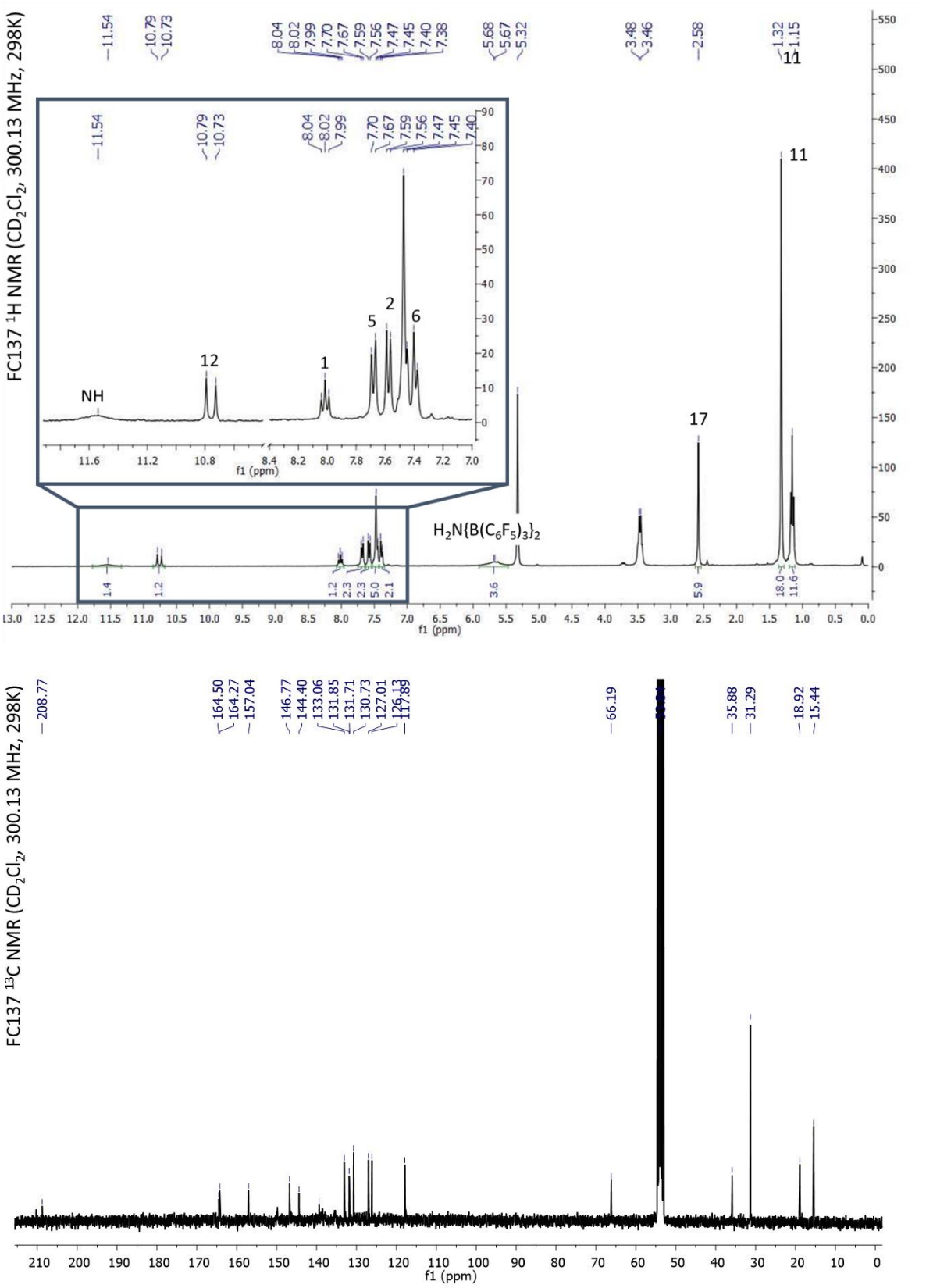

Figure S1.5: ^{1}HNMR (top) and $^{13}C\{^{1}H\}$ NMR (down) of complex [(L^{H})Au-(E, Z)-CHNHXyl]$NH_2\{B(C_6F_5)_3\}_2 \cdot 2\ Et_2O$ **4a** in CD_2Cl_2 at 298 K.

Synthesis of [(L^{OMe})Au-(*E, Z*)-CHNHXyl][$NH_2\{B(C_6F_5)_3\}_2$] · 2 Et_2O (4b)

To a solution of (L^{OMe})Au-(E)-CHNXyl in CD_2Cl_2 one equivalent of $H(OEt_2)_2AB_2$ is added what affords the quantitative formation of [(L^{OMe})Au-(E)-CHNHXyl]$NH_2\{B(C_6F_5)_3\}_2$

^{1}H NMR (CD_2Cl_2, 300.13 MHz, 298K): δ 12.19 (br,d, NH^E + NH^Z), 11.13 (d, ^3J = 11.5 Hz, H^{12Z}), 10.56 (d, ^3J = 18.6 Hz, H^{12E}), 7.71 (br, H^Z), 7.63 (d, ^3J = 8.2 Hz, H^{5E}), 7.54 (d, ^3J = 8.2 Hz, H^{5Z}), 7.48-7.42 (overlap of aromatic signals), 7.36 (d, ^3J = 7.5 Hz, H^{15E}), 7.28 (br, s, H^{8Z} ^{or} ^{2Z}), 7.12 (d, ^3J = 7.6 Hz, H^{15Z}), 7.01 (s, H^{2E}), 6.93 (s, H^{2Z}), 5.68 (br, s, 2H, $H_2N\{B(C_6F_5)_3\}_2$), 4.08 (s, H^{18E}), 4.04 (s, H^{18Z}), 2.55 (s, H^{17E}), 2.43 (s, H^{17Z}), 1.31 (s, $H^{11E+H11Z}$). Using the relative integration of the signals H^{17Z}/H^{17E} and H^{18Z}/H^{18E} we estimate a Z/E ratio of about 1/6. $^{13}C\{^1H\}$ NMR(CD_2Cl_2, 75.47 MHz, 298K): δ 209.61 (s, C^{12Z}), 208.89 (s, C^{12E}), 172.10 (s, C^{1E}), 165.80 (s, C^{9E}), 164.09 (s, C^{3E}), 156.72 (s, C^{13}), 149.79 (m, C^{C6F5}), 146.69 (s, C^7), 141.14 (m, C^{C6F5}), 139.61 (s, C^{4E}), 138.71 (m, C^{C6F5}), 137.86 (m, C^{C6F5}), 135.32 (m, C^{C6F5}), 132.96 (s, C^8), 131.86 (s, C^{15}), 131.45 (s, C^{14}), 130.55 (s, C^5), 126.41 (s, C^{6E}), 126.18 (s, C^{6Z}), 125.79 (s, C^{16E}), 125.50 (s, C^{16Z}), 103.70 (s, C^{2E}), 103.48 (s, C^{2Z}), 57.17 (s, C^{18E}), 35.78 (s, C^{10E}), 35.62 (s, C^{10Z}), 31.25 (s, C^{11E}), 31.15 (s, C^{11Z}), 20.08 (s, C^{17Z}), 18.88 (s, C^{17E}).

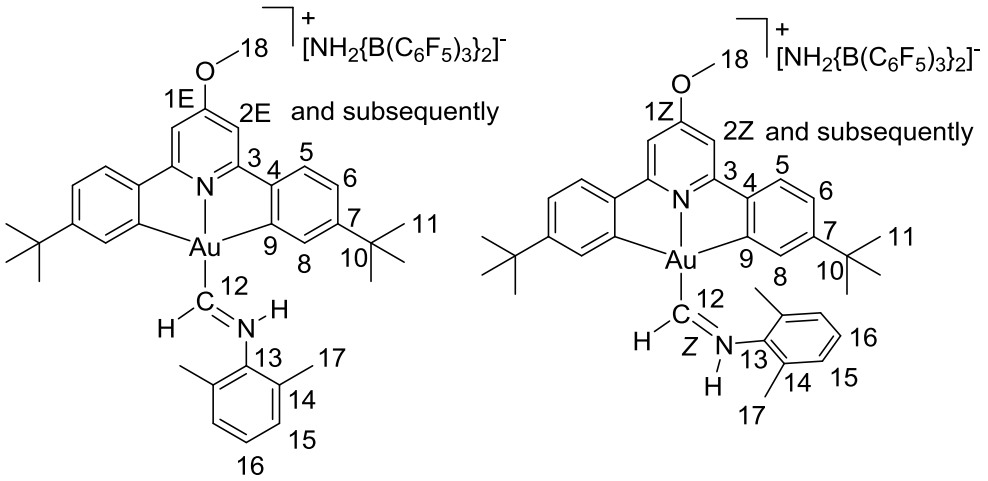

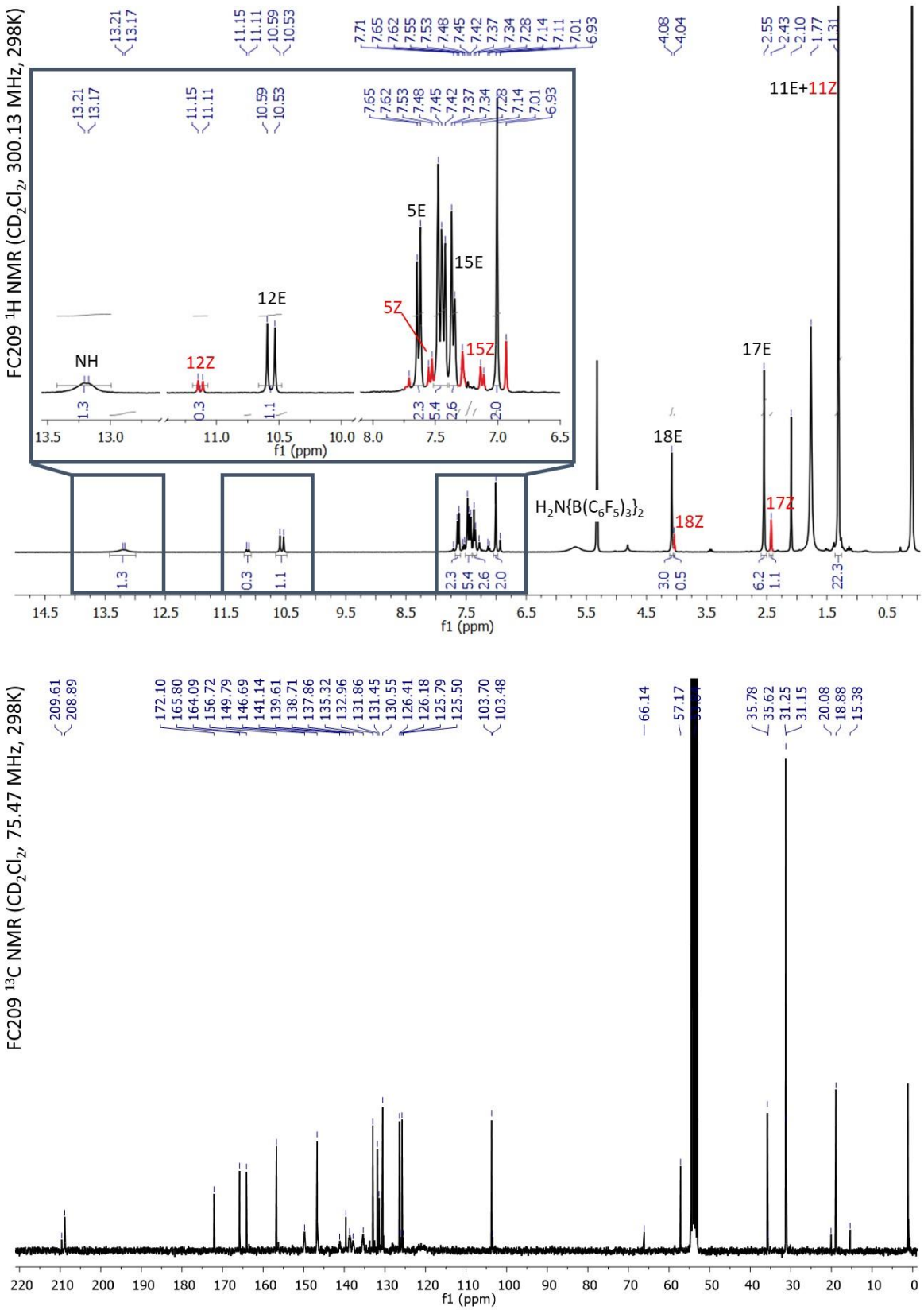

Figure S1.6: ^{1}HNMR (top) and ^{13}C{^{1}H} NMR (down) of complex [(L^{OMe})Au-(*E*, *Z*)-CHNHXyl]NH{B(C$_6$F$_5$)$_3$}$_2$ · 2 Et$_2$O **4b** in CD_2Cl_2 at 298 K.

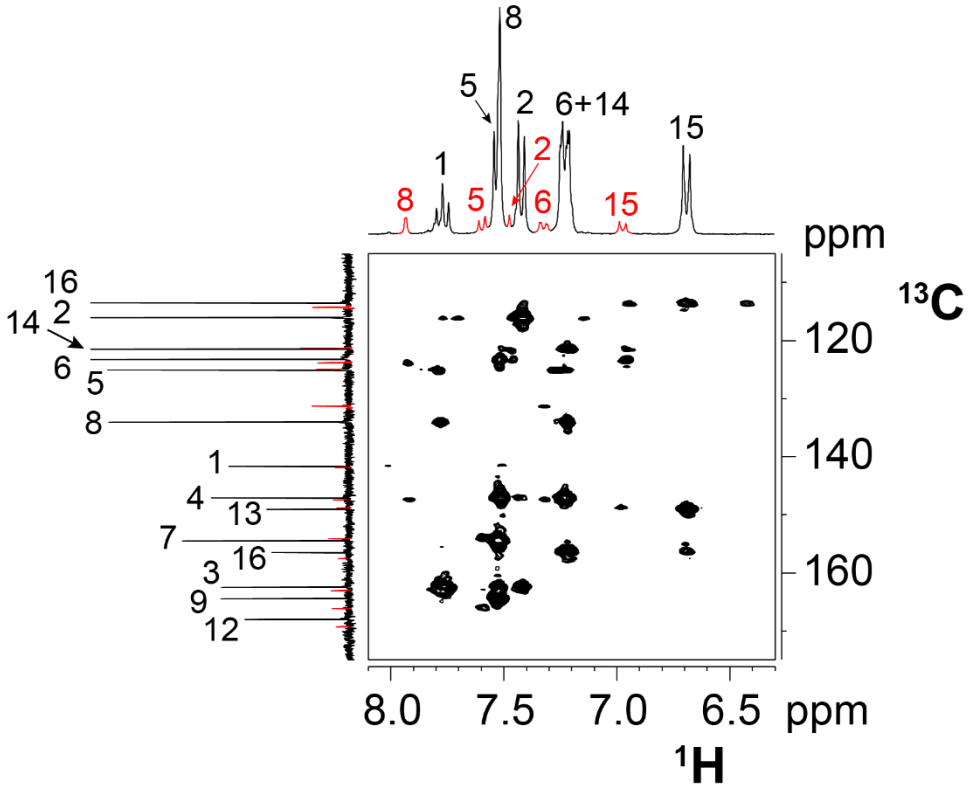

Figure S1.7. A section of the $^{1}H,^{13}C$ HMBC spectrum of **2a** (CD_2Cl_2, 297K). Signals due to the minor isomer are marked in red.

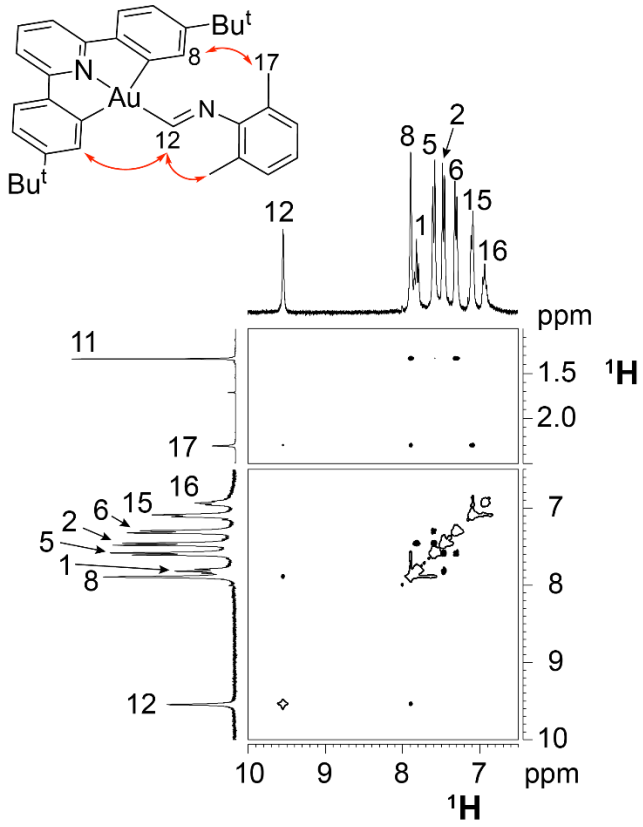

Figure S1.8 Two sections of the ^{1}H NOESY NMR spectrum of **1a** (CD_2Cl_2, 297K).

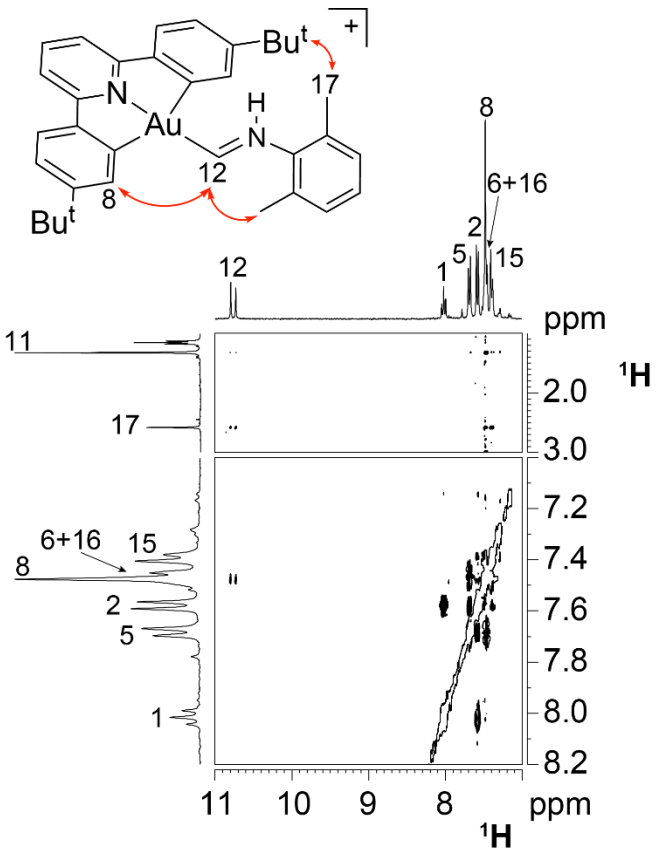

Figure S1.9 Two sections of the ^{1}H NOESY NMR spectrum of **4a** (CD_2Cl_2, 297K).

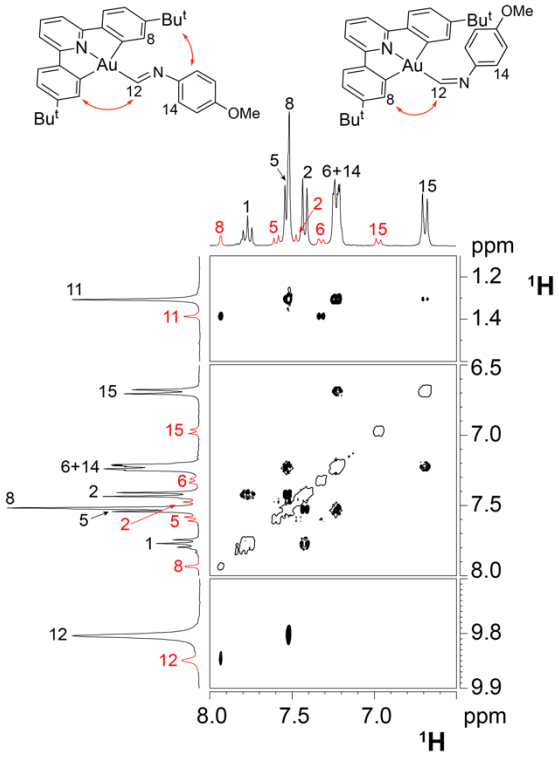

Figure S1.10 Three sections of the ^{1}H NOESY NMR spectrum of **2a** (CD_2Cl_2, 297K). Signals due to the minor isomer are marked in red.

Attempted insertion of N≡C-p-tol into (L^H)AuH

The same conditions described for 1a were employed but starting from (L^H)AuH (30 mg, 0.056 mmol), N≡CTol (ca. 8 mg, 0.5 mmol), and AIBN (ca. 0.2 eq.). (L^H)AuH (20 mg) was recovered. In a second attempt, the reaction mixture was heated up in toluene for 12 h. This evolves with the formation of a gold mirror and a complex mixture of organic products.

.

2. X-ray crystallography

At -30C, slow diffusion of Pentane in a saturated solution of of (L^{OMe})AuCHNXyl (**1b**) in Et_2O afforded colourless crystals of suitable quality for X-ray analysis. A block (0.5×0.2×0.2) was mounted in MiTeGen MicroMesh systems and fixed in the cold nitrogen stream on a diffractometer at 140 K. Diffraction intensities were recorded at 140 K on an Oxford Diffraction Xcalibur-3/Sapphire3-CCD diffractometer, equipped with Mo-Kα radiation and graphite monochromator. Data were processed using the CrystAlisPro-CCD and –RED software or CrystalClear-SM Expert 3.1 b27, been the absorption correction done at this stage.[S3]

The structure was determined by the direct methods routines with SHELXS and refined by full-matrix least-squares methods on F^2 in SHELXL.[S4] Non-hydrogen atoms were generally refined with anisotropic thermal parameters. Hydrogen atoms were included in idealised positions. Computer programs used in this analysis were run through WinGX.[S5] Scattering factors for neutral atoms were taken from reference S7. A brief summary of the most relevant parameters of the structure resolution and refine can be found in the Table below.

The structure was solved in the space group $P2_1/n$ and no missed symmetry was reported by PLATON.[S6] The asymmetric unit is formed by two molecules of the gold iminoformyl complexes and three molecules of Et_2O, what arises with the stoichiometry (L^{OMe})AuCHNXyl 1.5 Et_2O. Examination of the ΔMSDA values for the two possible isomers (L^{OMe})AuCH=NXyl *vs.* (L^{OMe})AuN=CHXyl supports our assignment as gold iminoformyl complex:

(L^{OMe})AuC27H=N2Xyl: C27 0.02159, N2 0.04236

(L^{OMe})AuC61H=N4Xyl: C61 0.02405, N4 0.03070 (Sum 0.1187)

(L^{OMe})AuN2=C27HXyl: C27 0.02522, N2 0.04253

(L^{OMe})AuN4=C61HXyl: C61 0.01636, N4 0.04136 (Sum 0.1255)

The check-cif reveals the presence of some alerts that must be addressed. The presence of residual electron density and positive voids generate two A-alerts but none of the peaks present any chemical meaning and are most likely arising from twining of the crystal. The refinement as merohedral twin improves somewhat the refinement but the alerts are still present. Also derived from this residual electron density the ADP max/min ratio for atom C70 has a large value. The presence of a peak of about 3 e^- near this atom suggests that this is due to a positional disorder of the group but modeling this disorder produces a worse refinement. Finally, the presence a large VOID in the Structure can be rationalized by the

presence of disordered crystallization solvent. In fact, one of the Et_2O molecules present a positional disorder that has been modeled. With the aim of improving the convergence of the model some reflections have been omitted and the restrictions EADP and ISOR have been used for reducing the thermal parameters of some atoms and to avoid some of them becoming non-positive-defined.

Table S2.1. Selected crystal data and structure refinement details for (L^{OMe})AuCHNXyl · 1.5 Et_2O **1b** · 1.5 Et_2O.

CCDC number 1860545.

Empirical formula	$C_{82}H_{106}Au_2N_4O_5$
F_w	1621.63
T (K)	140
crystal system, space group	monoclinic; P 21/n
a(Å)	13.7382(4)
b(Å)	33.2731(8)
c(Å)	18.3424(5)
α(deg)	90
β(deg)	110.790(3)
γ(deg)	90
volume (A^3)	7838.6(4)
Z	4
D_{calcd} (Mg/m^3)	1.374
absorption coefficient (mm^{-1})	3.789
F(000)	3296
θ range for data collection (deg)	2.93 to 27.103
no of data // restraints // params	17260 // 60 // 859
goodness-of-fit on $F^{2[a]}$	1.332
final R indexes $[I>2\sigma(I)]^{[a]}$	R1 = 0.067, wR2 = 0.1327
R indexes (all data)$^{[a]}$	R1 = 0.0775, wR2 = 0.137
largest diff peak and hole ($e.Å^{-3}$)	3.764 and -2.494

[a] $R1 = \Sigma(||F_o| - |F_c||)/\Sigma|F_o|$; $wR2 = [\Sigma w(F_o^2 - F_c^2)^2/\Sigma wF_o^2]^{1/2}$; goodness of fit = $\{\Sigma[w(F_o^2 - F_c^2)^2]/(N_{obs} - N_{param})\}^{1/2}$; $w = [\sigma^2(F_o) + (g_1P)^2 + g_2P]^{-1}$; $P = [\max(F_o^2;0 + 2F_c^2]/3$.

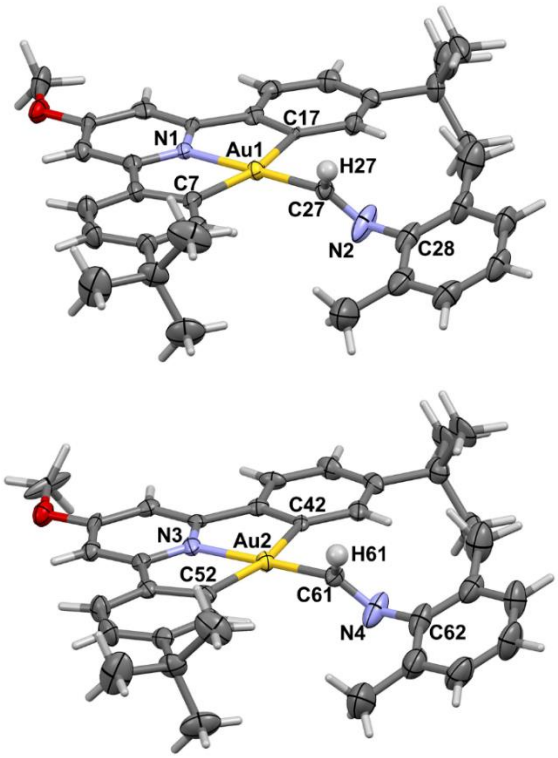

Figure S2.1: Structure of (L^{OMe})AuCHNXyl · 1.5 Et_2O (**1b** · 1.5 Et_2O). **Molecule A:** Au1-C27 2.005(7), Au1-C7 2.08(2), Au1-C17 2.075(7), Au1-N1 2.039(7), C27-N2 1.24(1), C27-H27 0.950, N2-C28 1.44(1), C17-Au1-N1 80.8(3), N1-Au1-C7 80.3(3), C7-Au1-C27 97.5(3), C27-Au1-C17 101.3(3), Au1-C27-N2 126.3(6), Au1-C27-H27 116.8, H27-C27-N2 116.9, C27-N2-C28 120.7(8). Angle between coordination plane of Au1 and Xyl ring 27.85º. **Molecule B:** Au2-C61 1.978(7), Au2-C42 2.081(7), Au2-N3 2.052(7), Au2-C52 2.071(9), C61-N4 1.25(1), N4-C62 1.43(1), C42-Au2-N3 80.6(3), N3-Au2-C52 80.5(3), C52-Au2-C61 97.3(3), C61-Au2-C42 101.7(3), Au2-C61-H61 116.1, Au2-C61-N4 128.1(7), C61-N4-C62 121.6(9). Angle between coordination plane of Au2 and Xyl ring 22.44º.

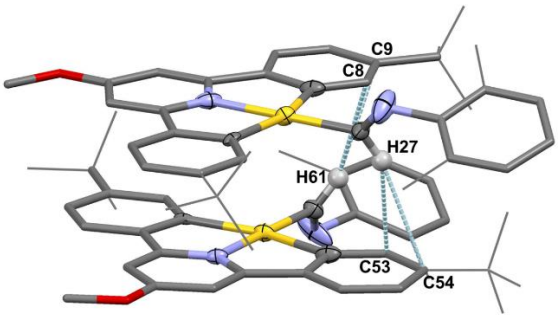

Figure S2.2: In the X-Ray structure of (L^{OMe})AuCHNXyl · 1.5 Et_2O (**1b** · 1.5 Et_2O) Molecule A and B pack together through the formation of hydrogen bonds. H27-C53 2.827, H27-C54 2.88, H61-C8 2.810, C61-C9 2.87.

3. Theoretical Calculations

Computational studies were performed for model systems lacking the *t*Bu substituents at the Au-bound phenyl rings. All calculations were done using Gaussian 09.[S8] Structures were optimized at the B3LYP[S9]/def2-SVP[S10] level (with a corresponding ECP at Au[S11]) for the gas phase. The nature of stationary points was checked by vibrational analyses. Improved single-point energies were obtained with M06[S12]/cc-pVTZ[S13] (and using the corresponding ECP at Au[S14]) including a PCM(Toluene) solvent correction.[S15] These were combined with the thermal corrections (enthalpy and entropy) at 298 K, 1 bar, obtained from the B3LYP/def2-SVP vibrational analyses. Entropy contributions to the free energy were scaled by a factor of 0.67 to account for reduced freedom in solution.[S16] Reaction profiles were evaluated for:

1. (C^N^C)AuH addition to xylyl isocyanide
2. (C^C^N)AuH addition to xylyl isocyanide
3. (C^N^C)AuH addition to 1-phenyl-propyne
4. the hypothetical (C^N^C)AuH addition to xylyl nitrile

Table S3.1 compares free energies for species along the three reaction paths; Table S3.2 contains all relevant total energies and corrections.

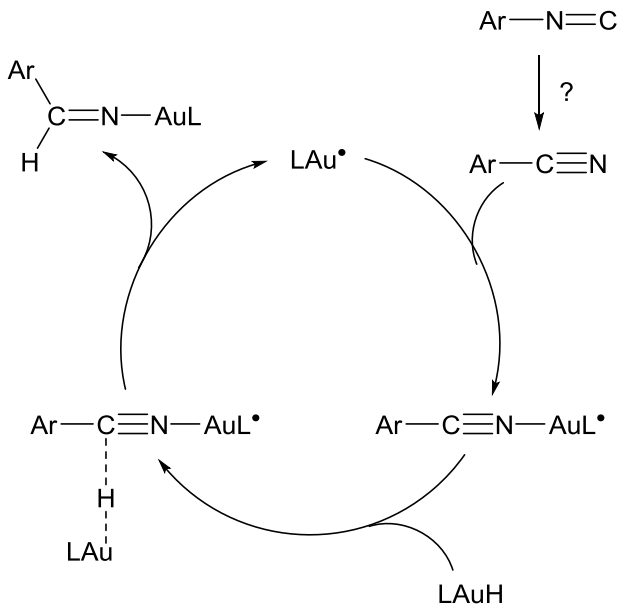

Figure S3.1. Hypothetical mechanism of catalyzed 1,2-addition of LAuH to xylylnitrile

Table S3.1. Gibbs free energies (298 K, 1 bar) for radical-mediated AuH additions to 1-phenyl propyne and xylylisocyanide (kcal/mol).

L:	C^N^C	C^N^C	C^C^N	C^N^C
Substrate:	MeC≡CPh	ArN≡C	ArN≡C	ArC≡N
LAu-AuL	-26.77	-26.77	-19.88	-19.88
LAu	0.00	0.00	0.00	(0)
bindTS	0.70	-	-	-
LAu.S	-4.48	-9.21	-13.14	+1.10
HtransTS	1.38	-2.06	-0.08	+16.50
LAuSH	-18.80	-7.83	-9.91	+14.71

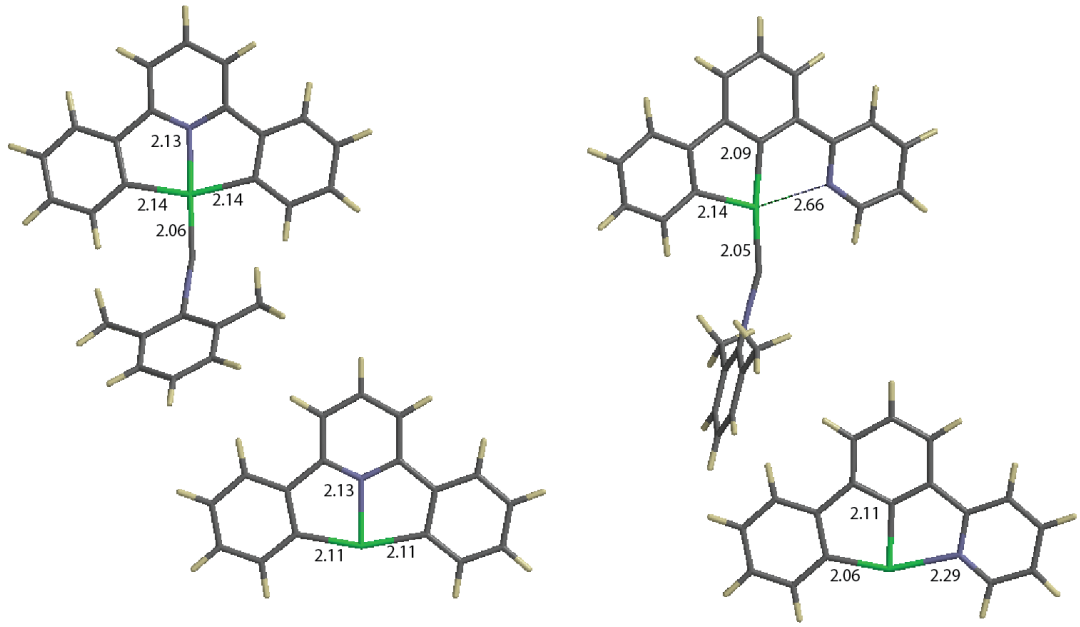

Fig. S3.2. Calculated structures of xylNC adducts of (C^N^C)Au(II) (left) and (C^C^N)Au(II) (right). Bond lengths in Å.

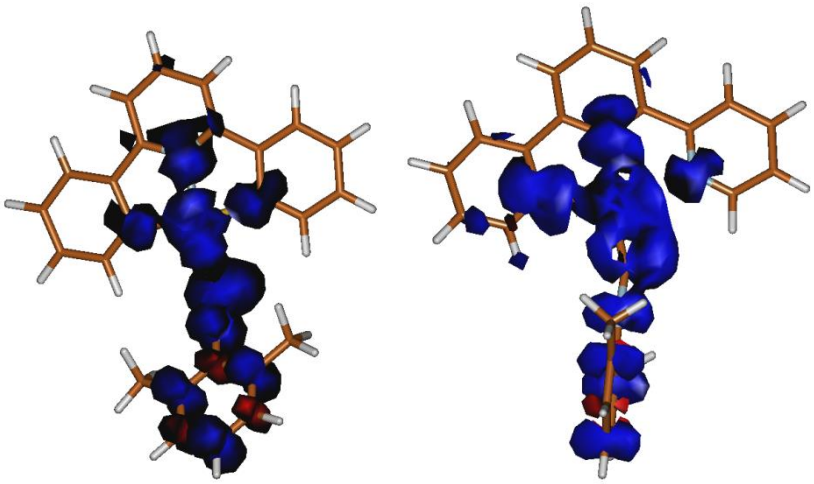

Fig S3.3 Spin density plots for (C^N^C)Au(CNxyl) (left) and (C^C^N)Au(CNxyl) (right).

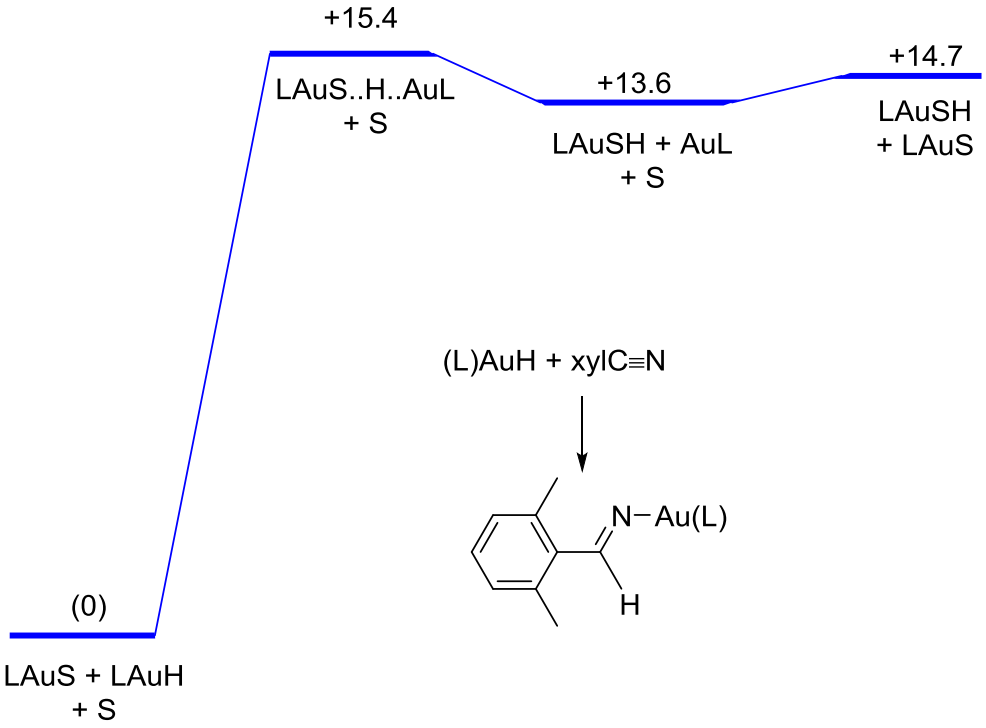

Figure S3.4. Calculated energy profile of the 1,2-addtion of (C^N^C)AuH to xylyl-C≡N (kcal/mol).

Table S3.2. Total and relative energies for addition of LAuH to 1-phenylpropyne and xylyl isocyanide.

Name	*H*corr	*TS*corr	*E*elec	$<S^2>$	*G*	*G* on scale [a]	*G*rel
(C^N^C)AuH + 1-phenylpropyne							
C2MePh	0.14692	0.04388	-347.55289	0.000	-347.43537		
CNCAuH	0.25278	0.05636	-845.20016	0.000	-844.98514		
CNCAu	0.24342	0.05670	-844.56888	0.753	-844.36344	***-2036.78396***	0.00
CNCAu_AuCNC [b]	0.48957	0.09451	-1689.23846	0.000	-1688.81222	-2036.82662	-26.77
CNCAu_C2MePh_bindTS	0.39084	0.08332	-1192.13272	0.759	-1191.79771	-2036.78285	0.70
CNCAu_C2MePh_trans	0.39135	0.08079	-1192.14318	0.786	-1191.80596	-2036.79110	-4.48
CNCAuC2MePh_HAuCNC_TS	0.64401	0.11862	-2037.34629	0.776	-2036.78176	-2036.78176	1.38
CNCAuC2MeHPh_trans	0.40450	0.07910	-1192.80197	0.000	-1192.45047	-2036.81391	-18.80
(C^N^C)AuH + xylyl isocyanide							
CNXyl	0.16386	0.04424	-402.91616	0.000	-402.78194		
CNCAuH	0.25278	0.05636	-845.20016	0.000	-844.98514		
CNCAu	0.24342	0.05670	-844.56888	0.753	-844.36344	***-2092.13053***	0.00
CNCAu_AuCNC [b]	0.48957	0.09451	-1689.23846	0.000	-1688.81222	-2092.17319	-26.77
CNCAu_CNXyl	0.40909	0.08386	-1247.51297	0.758	-1247.16006	-2092.14520	-9.21
CNCAu_CNXyl_HAuCNC_TS	0.66023	0.12299	-2092.71164	0.757	-2092.13381	-2092.13381	-2.06
CNCAuCHNXyl	0.42124	0.08309	-1248.14513	0.000	-1247.77956	-2092.14301	-7.83
CNCAuCHNXyl_copl	0.42123	0.08266	-1248.14514	0.000	-1247.77929	-2092.14274	-7.66
CNCAu_H_AuCNC	0.49563	0.09758	-1689.79278	0.756	-1689.36252	-2092.14446	-8.74
CNCAu_2_CNXyl [b]	0.65586	0.11676	-2092.17180	0.000	-2091.59416	-0.07066	-44.34
CNCAu_2_CNXyl2 [b]	0.65574	0.11743	-2092.17134	0.000	-2091.59428	-0.07077	-44.41
CNCAu_2_CNXyl_2 [b]	0.82295	0.13713	-2495.11250	0.000	-2494.38142	-0.06129	-38.46
CNCAu_2_CNXyl_22 [b]	0.82289	0.14035	-2495.12272	0.000	-2494.39386	-0.07373	-46.27
(C^C^N)AuH + xylyl isocyanide							
CNXyl	0.16386	0.04424	-402.91616	0.000	-402.78194		
CCNAuH	0.25221	0.05736	-845.19042	0.000	-844.97664		
CCNAu	0.24336	0.05840	-844.56611	0.758	-844.36188	***-2092.12046***	0.00
CCNAu_AuCCN [b]	0.48966	0.09572	-1689.21266	0.000	-1688.78713	-2092.15215	-19.88
CCNAu_CNXyl	0.40901	0.08826	-1247.51464	0.756	-1247.16476	-2092.14139	-13.14
CCNAu_CNXyl_HAuCCN_TSu	0.65926	0.12299	-2092.69286	0.759	-2092.11600	-2092.11600	2.80
CCNAu_CNXyl_HAuCCN_TSv	0.65920	0.12308	-2092.69233	0.758	-2092.11560	-2092.11560	3.05
CCNAu_CNXyl_HAuCCN_TSw	0.65932	0.12489	-2092.69598	0.760	-2092.12033	-2092.12033	0.08
CCNAu_CNXyl_HAuCCN_TSx	0.65935	0.12284	-2092.69763	0.760	-2092.12059	***-2092.12059***	-0.08
CCNAuCHNXyl	0.42126	0.08281	-1248.14015	0.000	-1247.77438	-2092.13626	-9.91
CCNAuCHNXyl_copl	0.42127	0.08268	-1248.14034	0.000	-1247.77448	-2092.13636	-9.98
(C^N^C)AuH + xylyl cyanide							
NCXyl	0.16432	0.04448	-402.94809	0.000	-402.81358		
CNCAuH	0.25278	0.05636	-845.20016	0.000	-844.98514		
CNCAu	0.24342	0.05670	-844.56888	0.753	-844.36344	***-2092.16216***	0.00
CNCAu_AuCNC	0.48957	0.09451	-1689.23846	0.000	-1688.81222	-2092.20483	-26.77

Name	***H*corr**	***TS*corr**	***E*elec**	**<S^2>**	***G***	***G* on scale [a]**	***G*rel**
CNCAu_NCXyl	0.40928	0.08793	-1247.52519	0.754	-1247.17483	-2092.15997	1.38
CNCAu_NCXyl2	0.40930	0.08866	-1247.52518	0.754	-1247.17527	-2092.16042	**1.10**
CNCAu_NCXyl_HAuCNC_TS	0.65997	0.12187	-2092.71419	0.759	-2092.13588	-2092.13588	**16.50**
CNCAu_NCXyl_HAuCNC_TS2	0.65998	0.12222	-2092.70854	0.761	-2092.13044	-2092.13044	19.91
CNCAuNCHXyl	0.42178	0.08299	-1248.14146	0.000	-1247.77527	-2092.13872	14.71

[a] LAu + LAuH + substrate; chosen reference value in bold. Free energies calculated as $G = E\text{elec} + H\text{corr} - 0.67\ TS\text{corr}$. [b] Radical recombination reactions: two Au units with 0, 1 or 2 bridging isocyanides.

4. References

S1. A. Pintus, L. Rocchigiani, J. Fernandez-Cestau, P. H. M. Budzelaar, M. Bochmann, *Angew. Chem. Int. Ed.* 2016, **55**, 12321–12324.

S2. S. J. Lancaster, A. Rodriguez, A. Lara-Sanchez, M. D. Hannant, D. A. Walker, D. L. Hughes, M. Bochmann, *Organometallics* 2002, **21**, 451 – 453.

S3. *Programs CrysAlisPro*, Oxford Diffraction Ltd., Abingdon, UK (2010)

S4. G. M. Sheldrick, *Acta Cryst.* 2008, **A64**, 112.

S5. L. J. Farrugia, J. Appl. Cryst. 2012, **45**, 849-854.

S6. A. L. Spek, (2006) PLATON – A Multipurpose Crystallographic Tool, Utrecht University, Utrecht, The Netherlands. A. L. Spek, *Acta Cryst.* 1990, **A46**, C34

S7 '*International Tables for X-ray Crystallography'*, Kluwer Academic Publishers, Dordrecht. Vol. C. 1992, pp. 500, 219 and 193.

S8. *Gaussian 09 B.01*: M. J. Frisch, G. W. Trucks, H. B. Schlegel, G. E. Scuseria, J. R. Cheeseman, G. Scalmani, V. Barone, B. Mennucci, G. A. Petersson, H. Nakatsuji, M. Caricato, X. Li, H. P. Hratchian, A. F. Izmaylov, J. Bloino, G. Zheng, J. L. Sonnenberg, M. Hada, M. Ehara, K. Toyota, R. Fukuda, J. Hasegawa, M. Ishida, T. Nakajima, Y. Honda, O. Kitao, H. Nakai, T. Vreven, J. A. J. Montgomery, J. E. Peralta, F. Ogliaro, M. Bearpark, J. J. Heyd, E. Brothers, K. N. Kudin, V. N. Staroverov, R. Kobayashi, J. Normand, K. Raghavachari, A. Rendell, J. C. Burant, S. S. Iyengar, J. Tomasi, M. Cossi, N. Rega, J. M. Millam, M. Klene, J. E. Knox, J. B. Cross, V. Bakken, C. Adamo, J. Jaramillo, R. Gomperts, R. E. Stratmann, O. Yazyev, A. J. Austin, R. Cammi, C. Pomelli, J. W. Ochterski, R. L. Martin, K. Morukuma, V. G. Zakrzewski, G. A. Voth, P. Salvador, J. J. Dannenberg, S. Dapprich, A. D. Daniels, O. Farkas, J. B. Foresman, J. V. Ortiz, J. Ciolowski and D. J. Fox, Gaussian, Inc., Wallingford CT, 2009

S9. (a) A. D. Becke, *J. Chem. Phys.*, 1993, **98**, 5648-5652. (b) A. D. Becke, *J. Chem. Phys.*, 1993, **98**, 1372-1377. (c) C. T. Lee, W. T. Yang and R. G. Parr, *Phys. Rev. B*, 1988, **37**, 785-789.

S10 F. Weigend and R. Ahlrichs, *Phys. Chem. Chem. Phys.*, 2005, **7**, 3297-3305.

S11 D. Andrae, U. Haussermann, M. Dolg, H. Stoll and H. Preuss, *Theor. Chim. Acta*, 1990, **77**, 123-141.

S12 Y. Zhao and D. G. Truhlar, *Theor. Chem. Acc.*, 2008, **120**, 215-241.

S13 (a) T. H. Dunning, *J. Chem. Phys.*, 1989, **90**, 1007-1023. (b) D. E. Woon and T. H. Dunning, *J. Chem. Phys.*, 1993, **98**, 1358-1371. (c) K. L. Schuchardt, B. T. Didier, T.

Elsethagen, L. S. Sun, V. Gurumoorthi, J. Chase, J. Li and T. L. Windus, *J. Chem. Inf. Model.*, 2007, **47**, 1045-1052. (d) D. Feller, *J. Comput. Chem.*, 1996, **17**, 1571-1586.

S14 (a) D. Figgen, G. Rauhut, M. Dolg and H. Stoll, *Chem. Phys.*, 2005, **311**, 227-244. (b) K. A. Peterson and C. Puzzarini, *Theor. Chem. Acc.*, 2005, **114**, 283-296.

S15 (a) S. Miertus and J. Tomasi, *Chem. Phys.*, 1982, **65**, 239-245. (b) S. Miertus, E. Scrocco and J. Tomasi, *Chem. Phys.*, 1981, **55**, 117-129. (c) G. Scalmani and M. J. Frisch, *J. Chem. Phys.*, 2010, **132**, 114110.

S16 (a) R. Raucoules, T. de Bruin, P. Raybaud and C. Adamo, *Organometallics*, 2009, **28**, 5358-5367; (b) S. Tobisch and T. Ziegler, *J. Am. Chem. Soc.*, 2004, **126**, 9059-9071.